Available online at www.sciencedirect.com

ScienceDirect

Solid State Nuclear Magnetic Resonance 33 (2008) 12–15

Solid State Nuclear Magnetic Resonance

www.elsevier.com/locate/ssnmr

Improved resolution and detection of ^{31}P–Tl J-couplings at 21 T in ^{31}P magic angle spinning NMR spectra of inorganic compounds containing Tl/Bi/P/S

Matthew A. Gave[a], Kermit M. Johnson[a], Mercouri G. Kanatzidis[b], David P. Weliky[a,*]

[a]*Department of Chemistry, Michigan State University, East Lansing, MI 48824, USA*
[b]*Department of Chemistry, Northwestern University, Evanston, IL 60208, USA*

Received 8 August 2007; received in revised form 31 October 2007
Available online 13 November 2007

Abstract

For crystalline compounds containing Tl, Bi, P, and S, greatly improved chemical shift resolution was observed in ^{31}P magic angle spinning spectra obtained at 21 T relative to spectra obtained at 9.4 T. In Hz units, the spectral linewidths were not strongly dependent on the applied field, which may be a result of a significant contribution to the linewidths from transverse relaxation. Comparison of the spectra at the two different fields confirmed that spectral splittings were due to two-bond phosphorus–thallium J-coupling. These results suggest that ultra-high field may be a useful tool to improve spectral resolution of spin $\frac{1}{2}$ nuclei in crystalline inorganic compounds.

Keywords: ^{31}P; Solid state NMR; High field NMR; Ultra-high field NMR; 900 MHz; J-coupling; Inorganic; Resolution; Chalcophosphate; Thiophosphate

The first examples of phosphorous–thallium J-couplings in the solid state were recently reported for crystalline compounds containing Tl, Bi, P, and Q (Q = S or Se). The detection of these couplings was based on comparisons of ^{31}P magic angle spinning NMR spectra at 9.4 and 7 T spectra and also on comparisons between ^{31}P NMR spectra of Tl- and non Tl-containing isomorphic analogs [1]. Fig. 1A and B respectively display the structures of $Tl_4Bi_2(PS_4)_2(P_2S_6)$ [2] and $TlBiP_2S_7$ which were two of the compounds in this class that exhibited these couplings. The $Tl_4Bi_2(PS_4)_2(P_2S_6)$ compound contained $[P_2S_6]^{4-}$ and $[PS_4]^{3-}$ units linked together in layers by coordinating Bi^{3+} ions. These layers were separated by layers of Tl^+ ions. The $TlBiP_2S_7$ compound contained $[P_2S_7]^{4-}$ units linked together in two-dimensional layers by coordinating Bi^{3+} ions with Tl^+ ions between the layers. These structures demonstrated that the detected 500–1600 Hz splittings were due to two-bond P–Tl couplings and such couplings were the first example of non-one-bond P–Tl couplings in either the liquid- or the solid-state.

Although there are seven known compounds containing Tl, Bi, P, and Q and eight known compounds containing K, Bi, P, and Q [3–9], only β-$TlBiP_2Se_6$/β-$KBiP_2Se_6$ and $TlBiP_2S_7$/$KBiP_2S_7$ are structurally isomorphic. Although the crystal structure is not yet fully refined for $Tl_3Bi(PS_4)_2$ [1], this compound is likely structurally similar to $K_3Bi(PS_4)_2$ [3]. It is somewhat surprising that there are only a few examples of structural isomorphism because Tl^+ and K^+ have similar ionic radii (i.e. 0.150 and 0.138 Å, respectively) [10]. Electronic structure calculations might provide insight into why the simple replacement $K^+ \rightarrow Tl^+$ is infrequently observed in the absence of a significant modification to the crystal structure. Splittings due to P–Tl J-couplings may be useful experimental parameters to validate these calculations.

In this note, ultra-high field (21 T) NMR spectra of three thallium bismuth thiophosphates are reported, along with a comparison to the previously obtained 9.4 T spectra. Besides providing additional confirmation of the P–Tl J-couplings, the 21 T spectra offered a significant enhancement of chemical shift resolution over the spectra collected at lower field.

Fig. 2 displays 9.4 and 21 T ^{31}P magic angle spinning spectra of three compounds: $Tl_4Bi_2(PS_4)_2(P_2S_6)$, $Tl_3Bi(PS_4)_2$,

---

*Corresponding author. Fax: +1 517 353 1793.
E-mail address: weliky@chemistry.msu.edu (D.P. Weliky).

0926-2040/$ - see front matter © 2007 Elsevier Inc. All rights reserved.
doi:10.1016/j.ssnmr.2007.11.002

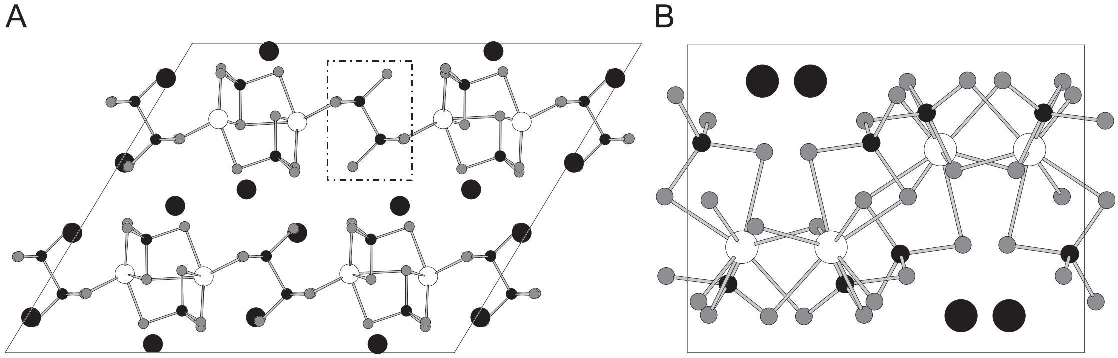

Fig. 1. (A) The structure of $Tl_4Bi_2(PS_4)_2(P_2S_6)$ viewed down the *b*-axis. Large black spheres are Tl, large hollow spheres are Bi, small black spheres are P, and small shaded spheres are S. A $[P_2S_6]^{4-}$ anion is highlighted in a dashed box. Two Tl^+ ions have been removed so that the highlighted $[P_2S_6]^{4-}$ unit is more clearly displayed. Two of the Ss in this unit are not visible because they are directly behind displayed Ss. (B) The structure of $TlBiP_2S_7$ viewed down the *c*-axis. Large black spheres are Tl, large hollow spheres are Bi, small black spheres are P, and small shaded spheres are S. A single unit cell is shown for each structure.

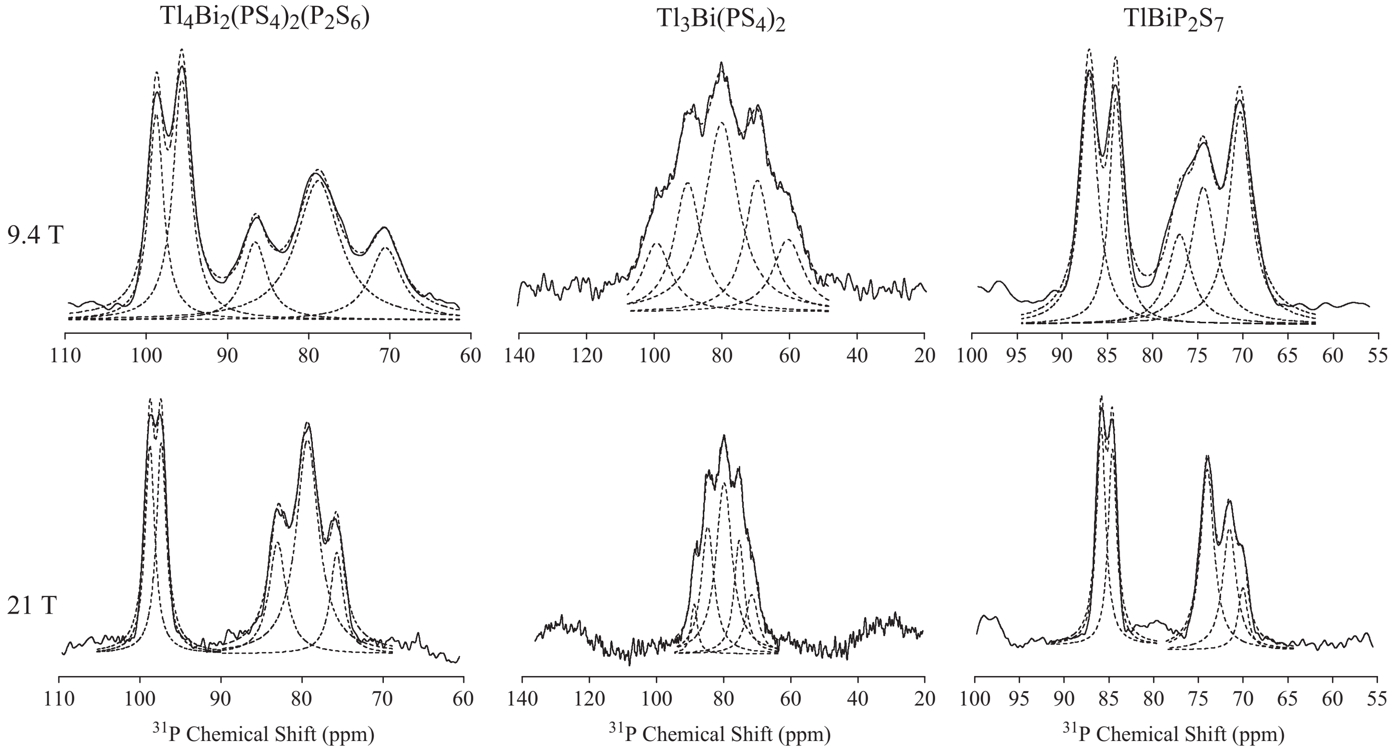
$Tl_4Bi_2(PS_4)_2(P_2S_6)$ $Tl_3Bi(PS_4)_2$ $TlBiP_2S_7$

Fig. 2. ^{31}P NMR spectra of $Tl_4Bi_2(PS_4)_2(P_2S_6)$, $Tl_3Bi(PS_4)_2$, and $TlBiP_2S_7$ obtained at 9.4 T (top) and 21 T (bottom). The experimental spectra are represented by solid lines and the best-fit Lorentzian functions used to deconvolve the spectra are represented by dashed lines. The sums of the Lorentzians are also shown as dashed lines and fitted well to the corresponding experimental spectra. Each spectrum was obtained at ambient temperature with magic angle spinning and was the sum of four Bloch decay scans. Pulse width calibration and chemical shift referencing were done with 85% H_3PO_4 (= 0 ppm). Each spectrum was processed identically with 50 Hz line broadening and baseline correction. Spectra at 9.4 T were collected on a Varian Infinity Plus spectrometer using a 4.0 mm magic angle spinning probe tuned to ^{31}P at 162.2 MHz. Other acquisition parameters were: 90° pulsewidth of 4.8 μs; transmitter at 0 ppm; spinning frequency of 14 kHz; and a recycle delay of 5000 s. Spectra at 21 T were collected on a Bruker AVANCE spectrometer using a 3.2 mm magic angle spinning probe tuned to ^{31}P at 364.3 MHz. Other acquisition parameters were: 90° pulsewidth of 10 μs; transmitter at −1.1 ppm; spinning frequency of 15 kHz; and recycle delay of 1000 s.

and $TlBiP_2S_7$. Each of the spectra could be fitted well to a sum of Lorentizian functions. In Fig. 2, the experimental spectra are displayed as solid lines, the individual Lorentzian functions are displayed as dotted lines, and the sums of the Lorentzian functions are also displayed as dotted lines. The spectra of $Tl_4Bi_2(PS_4)_2(P_2S_6)$ and $TlBiP_2S_7$ were separated into two clusters of Lorentzian peaks and the spectrum of $Tl_3Bi(PS_4)_2$ was a single cluster of Lorentzian peaks. Table 1 lists the peak shifts, linewidths, and integrated intensities of the fitted Lorentzians and Table 2 lists the average shift of each cluster of Lorentzian peaks as well as the splittings between adjacent Lorentzian peaks in the same cluster. For each compound, the consistency between the average shifts and the peak splittings at different fields confirmed that the

Table 1
Chemical shifts, linewidths, and integrated intensities of the fitted Lorentzian components of the spectra[a]

Compound	9.4 T			21 T		
	Peak shift (ppm)	Linewidth (Hz)[b]	Integrated intensity[c]	Peak shift (ppm)	Linewidth (Hz)[b]	Integrated intensity[c]
$Tl_4Bi_2(PS_4)(P_2S_6)$	99.8	350	51	98.8	520	42
	96.6	420	71	97.4	540	44
	87.6	570	31	83.0	910	40
	79.8	1040	100	79.3	1200	100
	71.5	760	38	75.7	700	27
$Tl_3Bi(PS_4)_2$	99.2	1600	31	88.7	750	11
	90.0	1490	54	84.7	1630	59
	80.0	1890	100	79.8	2060	100
	69.4	1410	52	75.3	1300	42
	60.3	1710	35	71.6	1610	27
$TlBiP_2S_7$	87.0	360	93	85.9	430	82
	84.1	290	66	84.6	390	67
	77.0	510	47	74.0	650	100
	74.4	530	74	71.5	640	67
	70.3	460	100	70.0	430	24

[a] Fitting of the Lorentzian functions was done with the OriginPro 7.5 program.

[b] The linewidth is the full-width at half-maximum of the Lorentzian peak function.

[c] The Lorentzian component with maximum integrated intensity was assigned a value of 100.

Table 2
Average chemical shifts and splittings of the spectral clusters

Compounds	Cluster identity	9.4 T		21 T	
		Shift (ppm)	Splitting (Hz)	Shift (ppm)	Splitting (Hz)
$Tl_4Bi_2(PS_4)(P_2S_6)$	Downfield doublet	98.2	520	98.1	510
	Upfield triplet	79.6	1270, 1350	79.3	1350, 1310
$Tl_3Bi(PS_4)_2$	Quintet	79.8	1600	80.0	1600
$TlBiP_2S_7$	Downfield doublet	85.6	470	85.3	470

splittings were likely due to ^{31}P–Tl J-couplings. Tl has two abundant isotopes with similar gyromagnetic ratios and splittings due to individual Tl isotopes were not resolved. The upfield clusters of the $TlBiP_2S_7$ spectra were not included in Table 2 because it was not possible to make an assignment with a consistent average shift and peak splitting at the two fields. This difficulty may have been due to overlapping peaks from unidentified impurities in the sample. Minor impurities were also apparent as additional peaks in the powder diffraction pattern.

There were two crystallographically inequivalent P in $Tl_4Bi_2(PS_4)_2(P_2S_6)$ and one P was associated with the $[PS_4]^{3-}$ unit and one P was associated with the $[P_2S_6]^{4-}$ unit. The downfield "doublet" exhibited much larger chemical shift anisotropy than did the upfield "triplet" and the doublet and triplet were assigned to the $[P_2S_6]^{4-}$ and $[PS_4]^{3-}$ units, respectively [1,11]. The ^{31}P in the $[P_2S_6]^{4-}$ and $[PS_4]^{3-}$ units had, respectively, five and six Tl separated by two bonds and the reason for the simple experimental splitting patterns was not obvious. The ratio of relative integrated intensities of the double and triplet was 0.72 at 9.4 T and 0.51 at 21 T. The 9.4 T result was closer to the 1.0 ratio expected from the crystal structure. The lower ratio observed at 21 T may be a result of: (1) a weaker RF field and larger transmitter offsets at 21 T with a consequent larger difference of the effective fields for the doublet and triplet; and (2) a shorter recycle delay at 21 T and the consequent effect of differential longitudinal relaxation for the doublet and triplet.

The spectra of $Tl_3Bi(PS_4)_2$ could be fitted as a quintet at both fields. The structure of this compound has not yet been fully refined. The compound $K_3Bi(PS_4)_2$ is isotypic and has a well-refined structure [1] that may be a reasonable model for the structure of $Tl_3Bi(PS_4)_2$. There are two crystallographically inequivalent P atoms in $K_3Bi(PS_4)_2$ and one ^{31}P has 10 K^+ separated by two bonds while the other ^{31}P has six K^+ ions separated by two bonds. The $Tl_3Bi(PS_4)_2$ quintet can not be trivially understood by the replacement of K^+ ions with Tl^+ ions in this structure.

The spectra of $TlBiP_2S_7$ contained two clusters of peaks. At both fields, the downfield cluster was fitted as a doublet and the upfield cluster was fitted as a triplet. There was some variation in the appearance and the fitting of the upfield regions at the two different fields. These variations were likely due to: (1) as-yet unidentified impurities in the samples; and (2) the shorter recycle delay used at 21 T and the consequent possible effects of differential longitudinal relaxation. There were two crystallographically inequivalent P in $TlBiP_2S_7$ and the most reasonable assignment was the downfield doublet as one ^{31}P and some part of the upfield triplet as the other ^{31}P.

Table 1 shows that the linewidths in Hz of the individual Lorentzian components were not strongly dependent on field strength. The splittings due to J-couplings in Hz were also independent of field and there was therefore similar appearance of individual clusters at the two fields. However, in ppm units, the total linewidth of a cluster was approximately inversely proportional to field, and this led to greatly improved resolution between clusters at 21 T, i.e., better chemical shift resolution. This enhanced resolution was particularly noteworthy for the compound $Tl_4Bi_2(PS_4)_2(P_2S_6)$ for which the doublet and triplet were completely resolved at 21 T.

Good spectral deconvolution with Lorentzian functions suggested that the linewidths were dominated by the transverse relaxation rate. Such dominance may hold for crystalline compounds that have small chemical shielding inhomogeneity at each site. In addition, T_2 may not vary strongly as a function of applied field strength if $T_2 \ll T_1$ [12]. This inequality was likely valid for these compounds. It has also been observed that the ^{31}P longitudinal relaxation rates of metal selenophosphates were linearly correlated with the squares of dipolar couplings to the ^{31}P [13]. These couplings are independent of magnetic field strength and could also contribute to the transverse relaxation rates of metal thiophosphates.

Motivations for ultra-high field magic angle spinning spectroscopy of solids have included improved resolution in spectra of biological macromolecules due to attenuation of broadening from ^{13}C to ^{13}C J-couplings [14], reduction of second-order quadrupolar broadening [15], and improved sensitivity [16]. The present study provides an example of greatly improved chemical shift resolution at 21 T for spin $\frac{1}{2}$ nuclei in crystalline inorganic solids. This improvement correlated with field-independent linewidths and splittings due to ^{31}P–Tl J-couplings. These splittings may be useful parameters for understanding the electronic structure of these compounds.

Access and assistance with the 900 MHz NMR was provided by Dr. Aizhuo Liu and by the Michigan Center for Structural Biology and financial support was provided by NSF DMR-0443783.

References

[1] M.A. Gave, C.D. Malliakas, D.P. Weliky, M.G. Kanatzidis, Inorg. Chem. 46 (2007) 3632–3644.

[2] M.A. McGuire, T.K. Reynolds, F.J. DiSalvo, Chem. Mater. 17 (2005) 2875–2884.

[3] T. McCarthy, M.G. Kanatzidis, J. Alloys Compds. 236 (1996) 70–85.

[4] T. McCarthy. Molten alkali metal polychalcogenide and polychalcophosphate salt synthesis of ternary and quaternary chalcogenides, Ph.D. Thesis, Michigan State University, East Lansing, MI, 1994.

[5] T.J. McCarthy, M.G. Kanatzidis, Chem. Mater. 5 (1993) 1061–1063.

[6] T.J. McCarthy, M.G. Kanatzidis, J. Chem. Soc. Chem. Commun. (1994) 1089–1090.

[7] J.D. Breshears, M.G. Kanatzidis, J. Am. Chem. Soc. 122 (2000) 7839–7840.

[8] V. Manriquez, A. Galdamez, D.R. Leon, M.T. Garland, M. Jimenez, Z. Krist. New Cryst. St. 218 (2003) 151–152.

[9] M.A. Gave, D.P. Weliky, M.G. Kanatzidis, Inorg. Chem., in press.

[10] N.N. Greenwood, A. Earnshaw, Chemistry of the Elements, second ed, Butterworth-Heinemann, Boston, MA, 1997 (pp. 75–222).

[11] C.G. Canlas, M.G. Kanatzidis, D.P. Weliky, Inorg. Chem. 42 (2003) 3399–3405.

[12] R.K. Harris, Nuclear Magnetic Resonance Spectroscopy, Longman Scientific and Technical, New York, NY, 1983, 87pp.

[13] C.G. Canlas, R.B. Muthukumaran, M.G. Kanatzidis, D.P. Weliky, Solid State Nucl. Magn. Reson. 24 (2003) 110–122.

[14] S.K. Straus, T. Bremi, R.R. Ernst, Chem. Phys. Lett. 262 (1996) 709–715.

[15] G.L. Hoatson, D.H.H. Zhou, F. Fayon, D. Massiot, R.L. Vold, Phys. Rev. B. 66 (2002) 224103-1.

[16] D. Marulanda, M.L. Tasayco, M. Cataldi, V. Arriaran, T. Polenova, J. Phys. Chem. B 109 (2005) 18135–18145.